J Mater Sci (2014) 49:6937–6943
DOI 10.1007/s10853-014-8398-6

Phase coexistence in $Bi_{1-x}Pr_xFeO_3$ ceramics

D. V. Karpinsky · I. O. Troyanchuk · V. Sikolenko · V. Efimov · E. Efimova · M. Willinger · A. N. Salak · A. L. Kholkin

Received: 22 April 2014 / Accepted: 11 June 2014 / Published online: 1 July 2014
© Springer Science+Business Media New York 2014

Abstract $Bi_{1-x}Pr_xFeO_3$ ceramics across the rhombohedral–orthorhombic phase boundary have been studied by X-ray diffraction, transmission electron microscopy, and differential scanning calorimetry. The structural phase transitions in $Bi_{1-x}Pr_xFeO_3$ driven by doping concentration and temperature are significantly different from those in $BiFeO_3$ compounds doped with other rare-earth elements. The features of the structural transformations have been discussed based on the specific character of the chemical bonds associated with praseodymium ions. The detailed study of the crystal structure evolution clarified the ranges of both single-phase and phase coexistence regions at different temperatures and dopant concentrations. For $x = 0.125$, compound extraordinary three-phase coexistence state has been observed in a narrow temperature range at about 400 °C. The results explicate driving forces of the structural transitions and elucidate the origin of the remarkable physical properties of $BiFeO_3$-based compounds near the morphotropic phase boundary.

D. V. Karpinsky (✉) · A. N. Salak · A. L. Kholkin
CICECO & Department of Materials and Ceramics Engineering, University of Aveiro, 3810-193 Aveiro, Portugal
e-mail: karpinski@ua.pt

D. V. Karpinsky · I. O. Troyanchuk
Scientific-Practical Materials Research Centre of NAS of Belarus, P. Brovka str. 19, 220072 Minsk, Belarus

V. Sikolenko
Helmholtz-Zentrum-Berlin for Materials and Energy, 14109 Berlin, Germany

V. Sikolenko · V. Efimov · E. Efimova
Joint Institute for Nuclear Research, Dubna 141980, Russia

M. Willinger
Abteilung Anorganische Chemie, Fritz-Haber-Institut der Max-Planck-Gesellschaft, Faradayweg 4-6, 14195 Berlin, Germany

A. L. Kholkin
Ural Federal University, Lenin Ave. 51, Ekaterinburg 620083, Russia

Introduction

Bismuth ferrite-based multiferroics of the compositions near doping-induced phase boundary attract renewed interest in the last years due to their remarkable physical properties and fundamental physics involved [1–3]. It is assumed that the crystal structure of the $BiFeO_3$ compounds doped with the rare-earth elements (viz. RE = La-Sm) is characterized by the following phase transition sequence: polar rhombohedral–anti-polar orthorhombic–non-polar orthorhombic phases. In spite of a large number of studies the mechanism of the structural transitions in $BiFeO_3$-based compounds near the morphotropic phase boundary (MPB) is still ambiguous and is the subject of the intensive discussions [3–6].

The most pronounced physical properties (viz. enhanced electromechanical response and remanent magnetization) were observed in lanthanum and praseodymium-substituted $BiFeO_3$ compounds with compositions near the polar rhombohedral (R)–anti-polar orthorhombic (O_2) phase boundary. The crystal structure of the $Bi_{1-x}La(Pr)_xFeO_3$ compounds within the R–O_2 phase boundary is characterized by the features specific either to La-or Pr-substitutions, viz. the incommensurately modulated crystal structure has been observed in the La-doped compounds only [7, 8]. In addition, both La-and Pr-substituted systems manifest isothermal structural transformation which was discussed in Ref [9, 10] in terms of the relaxation of non-equilibrium structural phase. Temperature evolution of the crystal

structure obtained for the Pr-doped compounds differs significantly from that observed for the compounds with other rare-earth ions. The most intriguing feature of the $Bi_{1-x}Pr_xFeO_3$ crystal structure has been observed near the transition to the non-polar orthorhombic phase where the coexistence of the rhombohedral and both orthorhombic phases has been suggested [7, 9, 11].

It is known that in thin films misfit strain imposed by a substrate can stabilize various phases as well as phase coexistence state [12, 13]. Different structural polymorphs (tetragonal, rhombohedral, monoclinic) as well as their coexistence can be realized in epitaxial $BiFeO_3$ films grown on $SrTiO_3/LaAlO_3$ substrates [14–16]. It is assumed that phase coexistence state allows to release the misfit occurred in the film–substrate interface [16]. The phase coexistence state has also been observed in rare-earth-doped $BiFeO_3$ films in the vicinity of temperature-driven structural transitions [14, 17]. The nature of the coexistence of these multiple polymorphs in highly strained $BiFeO_3$ and has been discussed in terms of formation of nanoscale domains [16, 18].

The present study is aimed at further clarification of the crystal structure of Pr-doped $BiFeO_3$ ceramics within the morphotropic phase boundary region. In this work, thermal phase stability and driving forces for temperature-induced structural transitions are investigated. The study is focused on the temperature evolution of the crystal structure of Pr-doped $BiFeO_3$ ceramics characterized by the coexistence of the structural phases at room temperature. Understanding the exact crystal structure of $BiFeO_3$-based compounds at the phase boundary and the factors determining structural stability of the compounds near the MPB are of fundamental interest and will bring forward practical perspectives of using functional materials with controlled physical properties.

Experimental

Ceramic samples of $Bi_{1-x}Pr_xFeO_3$ (molar dopant concentrations $x = 0.11$, 0.125, and 0.15) were prepared by the two-stage solid-state reaction [9]. High-purity oxides taken in a stoichiometric ratio were thoroughly mixed using a planetary ball mill (Retsch PM 200). The ceramics were synthesized at 930–1030 °C (synthesis temperature was increased with the dopant concentration) followed by a fast cooling down to room temperature. X-ray diffraction measurements were performed with a PANalytical X'Pert MPD PRO diffractometer (Cu-K_α radiation) equipped with an Anton Paar (HTK 16 N) heating stage. Diffraction data were analyzed by the Rietveld method using the FullProf software package [19]. Differential scanning calorimetry (DSC) was carried out with a Setaram SETSYS 16/18 instrument in a flowing air. High-resolution transmission electron microscopy (HRTEM) measurements have been performed using a FEI TITAN 80-300 microscope. Theoretical modeling based on the semi-empirical methods was performed using a HyperChem 8.0 software package [20].

Results and discussion

Concentration- and temperature-induced transitions

X-ray diffraction data of the $Bi_{1-x}Pr_xFeO_3$ compounds recorded at room temperature testify that the polar rhombohedral and the anti-polar orthorhombic phases coexist in the concentration range $0.11 \leq x \leq 0.15$. The crystal structure of $Bi_{0.89}Pr_{0.11}FeO_3$ compound at room temperature has been successfully refined assuming 90 % of the rhombohedral phase (R-phase, space group R3c) and 10 % of the orthorhombic phase (O_2-phase). The rhombohedral phase is the same as that observed in $Bi_{1-x}Pr_xFeO_3$ compounds with lower dopant concentration ($x < 0.11$) [9, 21]. The orthorhombic phase has been refined using *Pnam* space group with a lattice metric $\sqrt{2}a_p*2\sqrt{2}a_p*4a_p$ (a_p is the fundamental perovskite lattice parameter). In the orthorhombic lattice, the ions residing at A-and/or B perovskite positions are shifted along the *b*-axis in opposite directions thus forming an anti-polar order, similar to that observed in $PbZrO_3$ [8, 22]. Praseodymium doping apparently leads to the increase of the orthorhombic phase fraction, the amount of the rhombohedral phase proportionally being decreased. The $x = 0.125$ compound contains 25 % of the orthorhombic phase, whereas for the $x = 0.15$ compound, the O_2-phase is the dominant one and the amount of the rhombohedral phase is about 10 % at room temperature.

Structural analysis of the $Bi_{1-x}Pr_xFeO_3$ compounds across the phase boundary has been performed considering the phenomenon of isothermal structural transformation observed in the RE-doped $BiFeO_3$ ceramics [10]. The diffraction data discussed in this work have been obtained for the compounds left at room temperature for at least 2 months after synthesis, thus the crystal structure of the ceramics is supposed to be fully relaxed.

We have focused structural investigations on the temperature evolution of $Bi_{0.875}Pr_{0.125}FeO_3$ and $Bi_{0.85}Pr_{0.15}FeO_3$ compounds. The crystal structure of these compounds at room temperature is characterized by the coexistence of the R-and O_2-phases with the relative ratio (R:O_2) of 3:1 and 1:9, respectively. The temperature diffraction data obtained for the $x = 0.125$ compound demonstrate gradual decrease of the amount of the orthorhombic phase with temperature, whereas the fraction of the rhombohedral phase proportionally increases.

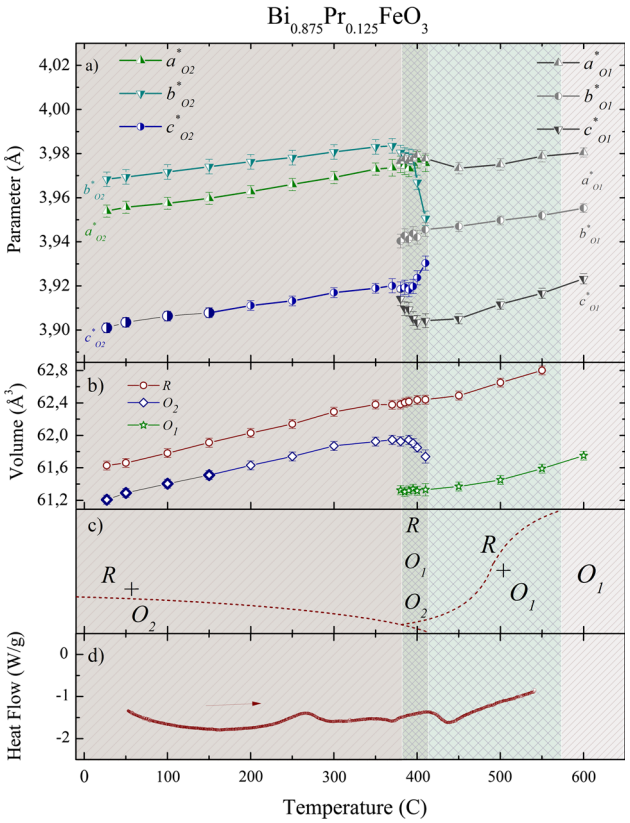

Fig. 1 Temperature evolution of the structural phases and lattice parameters of the $Bi_{0.875}Pr_{0.125}FeO_3$ compound: **a** unit cell parameters; **b** unit cell volumes; **c** phase evolution with temperature; **d** DSC data of the compound. The reduced quadrupled *c**-parameter of the anti-polar phase and the appropriate unit cell volume marks are depicted in *bold characters*

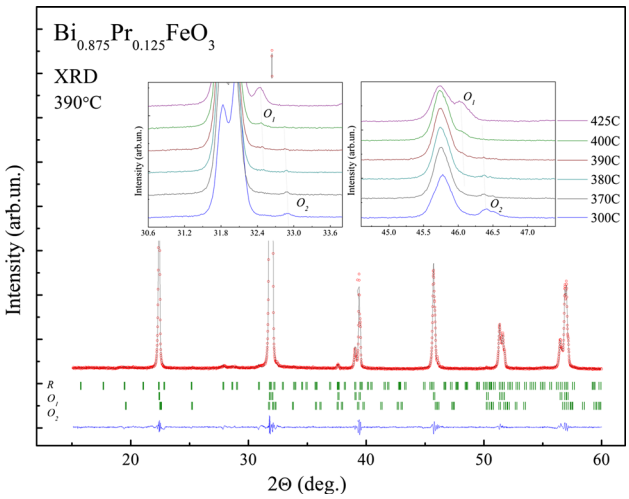

Fig. 2 The XRD pattern of the $Bi_{0.875}Pr_{0.125}FeO_3$ compound at 390 °C (*circles* are experimental data, *lines* are calculated ones). Bragg positions are indicated by *vertical ticks* (the rhombohedral phase, non-polar orthorhombic, anti-polar orthorhombic–from *top* to *bottom*). The *insets* show thermal evolution of the structural peaks characteristic for O_2-and O_1-phases

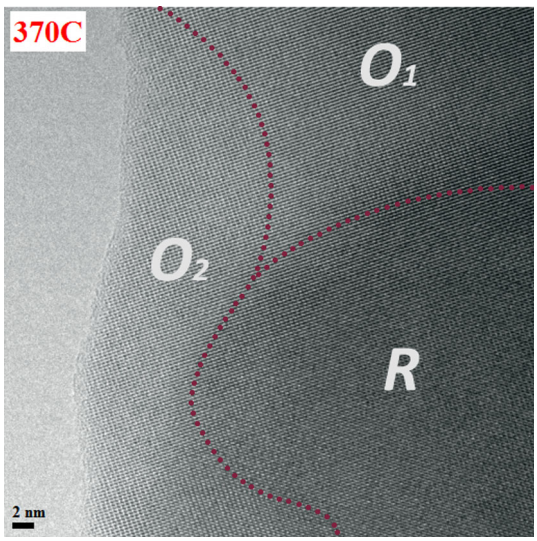

Fig. 3 HRTEM image of the $x = 0.125$ compound at $T = 370$ °C. The regions associated with different structural phases are delineated by *dashed lines*

The analysis of the XRD temperature data reveals a progressive increase of the lattice parameters of the $x = 0.125$ compound up to 350 °C whereas the diffraction peaks specific for the quadrupled c-parameter become negligible at about 150 °C. Above this temperature, the orthorhombic phase of the compound can be successfully described using *Pbam* space group with $\sqrt{2}a_p*2\sqrt{2}a_p*2a_p$ metric specific to the crystal structure of the $Bi_{1-x}Pr_xFeO_3$ compounds ($x > 0.25$) at room temperature (Fig. 1) [9, 21]. The amount of the orthorhombic phase gradually decreases with temperature and its fraction amounts to about 15 % at 350 °C. Above this temperature, the orthorhombic phase further diminishes, while the new orthorhombic phase (O_1) appears (Fig. 2) and can be successfully refined using a centrosymmetric *Pnma* space group. In the narrow temperature range around 390 °C, the coexistence of three structural phases (R, O_2, O_1) has been verified thus confirming the idea proposed in the previous study [23]. The concept of the three-phase coexistence state stable in the temperature range is thermodynamically self-consistent if one will consider non-equilibrium character of one structural phase. Time evolution of non-equilibrium structural state was discussed in Ref [10] where crystal structure of the La-substituted $BiFeO_3$ ceramics with compositions near the morphotropic phase boundary was studied.

The coexistence of the three structural phases at elevated temperatures has been confirmed by in situ heating experiments inside the TEM. Three structural phases can

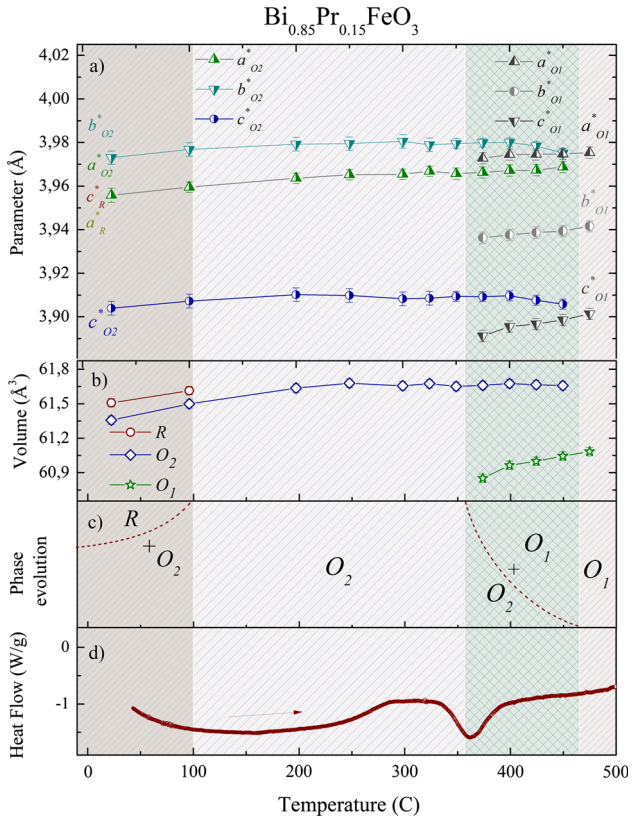

Fig. 4 Temperature evolution of the structural phases and lattice parameters of the $Bi_{0.85}Pr_{0.15}FeO_3$ compound: **a** unit cell parameters; **b** unit cell volumes; **c** phase evolution with temperature; **d** DSC data of the compound

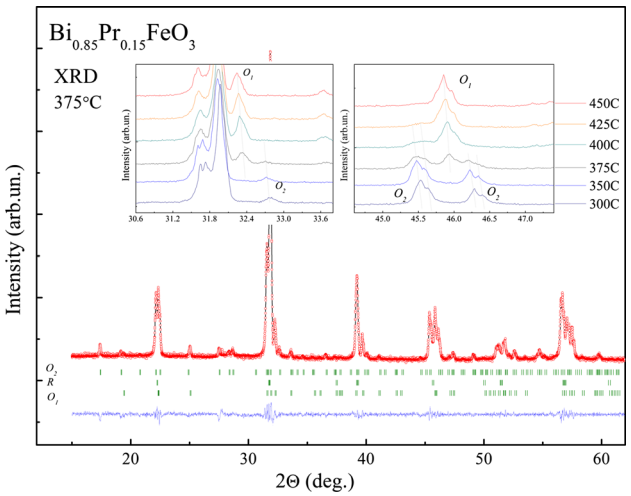

Fig. 5 The XRD pattern of the $Bi_{0.85}Pr_{0.15}FeO_3$ compound at 375 °C. Bragg positions are indicated by *vertical ticks* (the anti-polar orthorhombic phase, rhombohedral one, and non-polar orthorhombic—from *top* to *bottom*). The *insets* show thermal evolution of the structural peaks specific for different phases

be distinctively observed within one crystal grain with the size of about 40 nm (Fig. 3). The analysis of the FFT images obtained from the appropriate structural regions attested the structural phases estimated from the X-ray diffraction data. The HRTEM images obtained at different temperatures allowed to estimate temperature evolution of the mentioned structural phases, in particular lattice dynamics of the structural transformations in the $x = 0.125$ compound. The temperature region of the three-phase coexistence state estimated from the HRTEM data (300–500 °C) is significantly wider than that calculated based on the X-ray diffraction data and it can be explained by the local character of TEM measurements.

The evolution of the crystal structure across the three-phase coexistence region is thoroughly analyzed and presented in the next section. The anti-polar orthorhombic phase disappears slightly above 400 °C, while the amount of newly appeared non-polar orthorhombic phase rapidly increases. The unit cell parameters attributed to the rhombohedral and the non-polar orthorhombic structural phases gradually increase with temperature up to about 550 °C. Above this temperature, the rhombohedral phase vanishes and the single-phase state with non-polar orthorhombic structure stabilizes (Fig. 1).

Temperature evolution of the crystal structure calculated for the $Bi_{0.85}Pr_{0.15}FeO_3$ compound has significantly different behavior (Fig. 4). The fraction of the rhombohedral phase estimated for the compound (about 10 % at room temperature) continuously decreases with temperature. Above 100 °C, we could not detect any traces of the rhombohedral phase and the crystal structure can be considered as a single-phase orthorhombic one up to 350 °C. The XRD pattern recorded at 350 °C reveals new diffraction peaks with negligibly small intensity. These peaks were successfully refined within $\sqrt{2}a_p * 2a_p * \sqrt{2}a_p$ metric and prove the emergence of the new non-polar orthorhombic phase (Fig. 5).

The diffraction peaks attributed to the anti-polar phase disappear above 400 °C and the structural transformation to the non-polar phase is considered to occur within the temperature range of 350–400 °C. While careful analysis of the diffraction patterns reveals certain asymmetry of the peaks above 400 °C which attests the presence of the anti-polar orthorhombic phase in the compound up to 450 °C (Fig. 5). Above this temperature, the crystal structure is considered to be single-phase orthorhombic one and can be described using orthorhombic *Pnma* space group. It should be noted that the quadrupling of the c-parameter in the anti-polar phase remains up to the temperature of the structural transition to the non-polar orthorhombic phase, while in $Bi_{0.875}Pr_{0.125}FeO_3$ compound, it disappears around 150 °C.

Three-phase coexistence region

In order to clarify the structural peculiarities of the three-phase coexistence state observed for the $x = 0.125$ compound, we analyzed the temperature evolution of the crystal structure of the $x = 0.125$ and 0.15 compounds in the temperature range of 300–600 °C. In the temperature ranges of the expected structural transitions, the XRD patterns were recorded at 10 °C steps. Figures 1 and 4 demonstrate reduced structural parameters of the orthorhombic phases calculated in accordance with the appropriate lattice metric. The structural parameters do not represent real primitive perovskite unit cells of the structural phases, while graphically denote temperature evolution of two orthorhombic phases.

In the temperature range of 380–410 °C which has been estimated as the three-phase coexistence region for the $x = 0.125$ compound, the unit cell parameters attributed to both orthorhombic phases that quickly change (Fig. 1). Within the mentioned temperature interval, the b-parameter of the anti-polar orthorhombic phase reduces by about 0.5 %, the c-parameter notably increases (0.2 %), whereas the a-parameter slightly increases. Thus, the volume of the anti-polar unit cell is decreased by 0.3 % in this temperature range. It should be noted that reduction of the b-parameter is apparently associated with a decrease of the anti-polar displacement of the ions along the b-axis of the orthorhombic lattice. The anti-polar displacement is associated with b/2a ratio which gradually decreases with temperature down to unity at about 410 °C.

In the temperature interval 380–410 °C, the unit cell parameters of the non-polar orthorhombic phase change quite slowly. The b-parameter slightly increases, the c-parameter shows an opposite trend and decreases by about 0.3 %, the a-parameter demonstrates only small decrease, thus the related unit cell volume remains nearly constant. The unit cell volume of the rhombohedral phase gradually expands in the temperature range of 380–410 °C.

Analysis of the structural evolution of the anti-polar and the non-polar orthorhombic phases within the three-phase region in the $x = 0.125$ compound permitted to clarify the mechanism of the phase transition in the Pr-doped $BiFeO_3$ ceramics. As was mentioned above, the XRD data for the $x = 0.125$ compound suggest gradual reduction of the anti-polar order with temperature increase and its disruption ends up at about 410 °C. The transformation from the anti-polar structure to the non-polar one is accompanied by a modification of the unit cell lattice wherein the b-parameter (indicative for the anti-polar order) in O_2-phase is decreased by two times and its value becomes close to the c-parameter in the O_1-phase. The c-parameter in the O_2-phase demonstrates opposite trend and rapidly increases in the temperature range of 390–410 °C becoming close to the b-parameter of the O_1-phase. The a-parameter of the O_2-phase remains nearly constant within the above-mentioned temperature range, and its value is almost equal to that of the a-parameter of the O_1-phase.

Considering the described structural changes, the most probable scenario of the phase transition assumes a transformation of the anti-polar structure into the non-polar one associated with a decrease of the unit cell volume of about 1 %. This transformation is in accordance with the group–subgroup relation between the appropriate space groups *Pbam* (#55) and *Pnma* (#62). Taking onto account, the number of formula units per primitive unit cell for these space groups (8 and 4 for *Pbam* and *Pnma*, correspondingly) and the equality of the orders of the related point groups, one can consider one step transformation *Pbam* → *Pnma* with the transformation index $i = 2$.

The difference between the temperature-induced structural transitions in the $x = 0.125$ and $x = 0.15$ compounds

It should be noted that the structural transformation into the non-polar orthorhombic state observed in the Pr-doped compounds is significantly different from those attested for $BiFeO_3$ compounds doped with other rare-earth elements [7, 9, 11, 24]. In the La-doped compound with similar phase ratio (at room temperature), the above-mentioned structural transition occurs via formation of the single-phase state with rhombohedral symmetry [8, 9, 23]. Different characters of the structural transition observed in the La-and Pr-doped compounds are confirmed by DTA/TG measurements [8, 25] which testify the absence of any distinct anomaly in the Pr-doped compounds as compared with analogous La-doped $BiFeO_3$ compounds. Taking into account the DTA/TG and diffraction data available for the La-and Pr-doped compounds, one may suggest that it is the specific character of the Pr–O chemical bonds that determines distinctive structural transition in the $Bi_{0.875}Pr_{0.125}FeO_3$. The distinct character of the Pr–O chemical bonds is most probably associated with higher covalent component. The estimation of the electron density distributions performed for Bi(Pr)–O chemical bonds in the rhombohedral phase testifies minimum electron densities values to be 0.5 and 0.3 $Å^{-3}$ for the Bi(Pr)–O bonds which determine polar order. The obtained values are close to those calculated in bismuth ferrite and significantly larger than values estimated for La-doped compounds [23, 26].

The analysis of the temperature evolution of the crystal structure testifies significantly different characters of the structural transition to the non-polar orthorhombic phase occurred in the $x = 0.125$ and $x = 0.15$ compounds. In the temperature range 100–380 °C, i.e., below the transition temperature, the crystal structure of the $Bi_{0.85}Pr_{0.15}FeO_3$

compound has been successfully refined assuming single-phase anti-polar orthorhombic structure. The transformation of the anti-polar orthorhombic phase can be described by the model proposed for the $x = 0.125$ compound, and the changes of the unit cell parameters calculated for the $x = 0.15$ compound are similar to those estimated in the $x = 0.125$ compound. Within the temperature range of the phase transition, the b-and c-parameters are decreased by $\sim$0.15 %, the a-parameter remains nearly constant and follows the trend observed in the $Bi_{0.875}Pr_{0.125}FeO_3$. The significant difference between the b-parameter of the O_2-phase and the related c-parameter of the O_1-phase ($\sim$2.5 %) as well as between the c-parameter of the O_2-phase and b-parameter of the O_1-phase of ($\sim$1.1 %) resulted in the decrease of the orthorhombic unit cell volume of $\sim$1.1 % (Fig. 4) which is less than the change of the relevant unit cell volume in the $x = 0.125$ compound ($\sim$1.9 %).

The difference in the structural transition is confirmed by DSC data which testify notable anomaly at about 360 °C (Fig. 4d) unlike the $x = 0.125$ compound (Fig. 1d). The anomaly at 360 °C is associated with the structural transformation from the anti-polar into the non-polar orthorhombic phase, while similar transition in $x = 0.125$ compound occurs near 380 °C which is close to the magnetic transition temperature [9, 21]. The anomaly observed in the DSC curves of the $x = 0.125$ compound is proportionally less pronounced than that in the $x = 0.15$ one and correlates well with the estimated phase ratio. The structural transition from the polar rhombohedral phase into the non-polar orthorhombic phase occurs in the $x = 0.125$ compound about 440 °C and has smaller heat transfer as compared with the transition between the orthorhombic phases (Figs. 1d, 4d). It should be noted that around 440 °C, the R–O_1 phase transition occurred in the $x = 0.125$ compound proceeds much faster as confirmed by the temperature XRD measurements. Comparing the crystal structure evolution of the $x = 0.125$ and $x = 0.15$ compounds, one can deduce that the dominant amount of the rhombohedral phase facilitates the formation of the phase coexistence state. The prevailing amount of the R-phase designed in the $x = 0.125$ compound has resulted in the three-phase coexistence region observed at the elevated temperatures. The structural state with coexisting rhombohedral and anti-polar orthorhombic phases is associated with increased mechanical compliance resulted in enhanced elastic and piezoelectric properties of the compounds as confirmed by the Piezoresponse Force Microscopy measurements in $Bi_{1-x}Pr_xFeO_3$ [9, 27]. Enhanced electromechanical properties have also been detected in $Bi_{1-x}RE_xFeO_3$ compounds series (RE = La, Nd, Sm) for the compositions near the morphotropic phase boundary [5, 28].

Conclusions

We studied temperature- and composition-driven structural transitions in $Bi_{1-x}Pr_xFeO_3$ ceramics with compositions within the phase boundary between the rhombohedral polar and orthorhombic anti-polar phases. Thermal diffraction data allowed delineating the single-phase and phase coexistence regions. The three-phase coexistence region has been confirmed in $Bi_{0.875}Pr_{0.125}FeO_3$ compound using both X-ray diffraction and TEM data. The specific character of the structural transitions occurred in the studied Pr-doped $BiFeO_3$ ceramics and, in particular, in the $x = 0.125$ compound has been discussed assuming special character of the Pr–O chemical bonds and decisive role of the rhombohedral phase causing high mechanical compliance of the compounds near the phase transition. Low structural stability of the rhombohedral phase estimated for the $x = 0.125$ compound with dominant rhombohedral phase results in the enhanced electromechanical properties of the ceramics near the phase boundary. The obtained results clarified the origin of driving forces of the structural phase transitions and define the phase coexistence conditions which may significantly improve physical properties of $BiFeO_3$-based ceramic materials.

Acknowledgements The authors would like to acknowledge the FCT (Grants SFRH/BPD/42506/2007, EXPL/CTM-NAN/1611/2013), RFFI (Grant 13-02-90903) and BRFFI (F014D-001). The work at CICECO was partly supported by the FCT Grant Pest-C/CTM/LA0011/013. Dr. Maria Celeste Azevedo is acknowledged for the DSC measurements.

References

1. Kan D, Palova L, Anbusathaiah V, Cheng CJ, Fujino S, Nagarajan V, Rabe KM, Takeuchi I (2010) Universal behavior and electric-field-induced structural transition in rare-earth-substituted $BiFeO_3$. Adv Funct Mater 20:1108–1115
2. Chu YH, Zhan Q, Yang C-H, Cruz MP, Martin LW, Zhao T, Yu P, Ramesh P, Joseph PT, Lin IN, Tian W, Schlom DG (2008) Low voltage performance of epitaxial $BiFeO_3$ films on Si substrates through lanthanum substitution. Appl Phys Lett 92:102909–102911
3. Yuan GL, Or SW, Liu JM, Liu ZG (2006) Structural transformation and ferroelectromagnetic behavior in single-phase $Bi_{1-x}Nd_xFeO_3$ multiferroic ceramics. Appl Phys Lett 89:052905–052907
4. Chen X, Hu G, Wu G, Yang C, Wang C, Fan S (2010) Large piezoelectric coefficient in Tb-doped $BiFeO_3$ films. J Am Ceram Soc 93:948–950
5. Karpinsky DV, Troyanchuk IO, Vidal JV, Sobolev NA, Kholkin AL (2011) Enhanced ferroelectric, magnetic and magnetoelectric properties of $Bi_{1-x}Ca_xFe_{1-x}Ti_xO_3$ solid solutions. Solid State Commun 151:536–540
6. Le Bras G, Bonville P, Colson D, Forget A, Genand-Riondet N, Tourbot R (2011) Effect of La doping in the multiferroic compound $BiFeO_3$. Phys B 406:1492–1495
7. Karpinsky DV, Troyanchuk IO, Mantytskaya OS, Khomchenko OS, Kholkin AL (2011) Structural stability and magnetic

properties of $Bi_{1-x}La(Pr)_xFeO_3$ solid solutions. Solid State Commun 151:1686–1689
8. Rusakov DA, Abakumov AM, Yamaura K, Van Belik AA, Tendeloo G, Takayama-Muromachi E (2010) Structural evolution of the $BiFeO_3$−$LaFeO_3$ system. Chem Mater 23:285–292
9. Troyanchuk IO, Karpinsky DV, Bushinsky MV, Mantytskaya OS, Tereshko NV, Shut VN (2011) Phase transitions, magnetic and piezoelectric properties of rare-earth-substituted $BiFeO_3$ ceramics. J Am Ceram Soc 94:4502–4506
10. Troyanchuk IO, Karpinsky DV, Bushinsky MV et al (2011) Isothermal structural transitions, magnetization and large piezoelectric response in $Bi_{1-x}La_xFeO_3$ perovskites. Phys Rev B 83:054109–054115
11. Khomchenko VA, Karpinsky DV, Kholkin AL et al (2010) Rhombohedral-to-orthorhombic transition and multiferroic properties of Dy-substituted $BiFeO_3$. J Appl Phys 108:074109–074113
12. Zhang JX, He Q, Trassin M et al (2011) Microscopic origin of the giant ferroelectric polarization in tetragonal-like $BiFeO_3$. Phys Rev Lett 107:147602–147605
13. Jang HW, Ortiz D, Baek S-H et al (2009) Domain engineering for enhanced ferroelectric properties of epitaxial (001) $BiFeO_3$ thin films. Adv Mater 21:817–823
14. Beekman C, Siemons W, Ward TZ et al (2013) Phase transitions, phase coexistence, and piezoelectric switching behavior in highly strained $BiFeO_3$ films. Adv Mater 25:5561–5567
15. Chen Z, Prosandeev S, Luo ZL et al (2011) Coexistence of ferroelectric triclinic phases in highly strained $BiFeO_3$ films. Phys Rev B 84:094116–094121
16. Emery SB, Cheng C-J, Kan D et al (2010) Phase coexistence near a morphotropic phase boundary in Sm-doped $BiFeO_3$ films. Appl Phys Lett 97:152902–152904
17. Wolter S, Michael DB, Joong Hee N, Hans MC (2011) Temperature-driven structural phase transition in tetragonal-like $BiFeO_3$. Appl Phys Expr 4:095801–095804
18. Cheng CJ, Kan D, Lim SH et al (2009) Structural transitions and complex domain structures across a ferroelectric-to-antiferroelectric phase boundary in epitaxial Sm-doped $BiFeO_3$ thin films. Phys Rev B 80:014109–014119
19. Rodriguez-Carvajal J (1993) Recent advances in magnetic structure determination by neutron powder diffraction. Phys B 192:55–69
20. Coleman WF, Arumainayagam CR (1998) HyperChem 5 (by Hypercube, Inc.). J Chem Educ 75:416
21. Khomchenko VA, Troyanchuk IO, Karpinsky DV, Paixao JA (2012) Structural and magnetic phase transitions in $Bi_{1-x}Pr_xFeO_3$ perovskites. J Mater Sci 47:1578–1581. doi:10.1007/s10853-011-6040-4
22. Teslic S, Egami T (1998) Atomic structure of $PbZrO_3$ determined by pulsed neutron diffraction. Acta Cryst B 54:750–765
23. Karpinsky DV, Troyanchuk IO, Tovar M et al. (2014) Temperature and composition-induced structural transitions in $Bi_{1-x}La(Pr)_xFeO_3$ ceramics. J Am Ceram Soc. doi: 10.1111/jace.12978
24. Levin I, Tucker MG, Wu H et al (2011) Displacive phase transitions and magnetic structures in Nd-substituted $BiFeO_3$. Chem Mater 23:2166–2175
25. Karpinsky DV, Troyanchuk IO, Tovar M, Sikolenko V, Efimov V, Kholkin AL (2013) Evolution of crystal structure and ferroic properties of La-doped $BiFeO_3$ ceramics near the rhombohedral–orthorhombic phase boundary. J. Alloys Compd 555:101–107
26. Fujii K, Kato H, Omoto K, Yashima M, Chen J, Xing X (2013) Experimental visualization of the Bi–O covalency in ferroelectric bismuth ferrite ($BiFeO_3$) by synchrotron X-ray powder diffraction analysis. Phys Chem Chem Phys 15:6779–6782
27. Panwar N, Coondoo I, Tomar I, Kholkin I, Puli VS, Katiyar RS (2012) Nanoscale piezoresponse and magnetic studies of multiferroic Co and Pr cosubstituted BFO thin films. Mater Res Bull 47:4240–4245
28. Karpinsky DV, Troyanchuk IO, Sikolenko V, Efimov V, Kholkin AL (2013) Electromechanical and magnetic properties of $BiFeO_3$–$LaFeO_3$–$CaTiO_3$ ceramics near the rhombohedral-orthorhombic phase boundary. J Appl Phys 113:187218–187223